cells

MDPI

Article

Serotonin Receptor 5-HT$_{2A}$ Regulates TrkB Receptor Function in Heteroreceptor Complexes

Tatiana Ilchibaeva [1,2,*], Anton Tsybko [2], Andre Zeug [1], Franziska E. Müller [1], Daria Guseva [3], Stephan Bischoff [3], Evgeni Ponimaskin [1,*] and Vladimir Naumenko [2]

[1] Cellular Neurophysiology, Center of Physiology, Hannover Medical School, Carl-Neuberg Strasse 1, 30625 Hannover, Germany; zeug.andre@mh-hannover.de (A.Z.); mueller.franziska@mh-hannover.de (F.E.M.)
[2] Laboratory of Behavioral Neurogenomics, Federal Research Center Institute of Cytology and Genetics, Siberian Branch of Russian Academy of Sciences, Prospekt Lavrentyeva 10, 630090 Novosibirsk, Russia; antontsybko@bionet.nsc.ru (A.T.); naumenko2002@mail.ru (V.N.)
[3] Department of Nutritional Medicine, University of Hohenheim, Fruwirthstr. 12, 70599 Stuttgart, Germany; daria.guseva@uni-hohenheim.de (D.G.); bischoff.stephan@uni-hohenheim.de (S.B.)
* Correspondence: ilchibaeva@bionet.nsc.ru (T.I.); ponimaskin.evgeni@mh-hannover.de (E.P.)

Abstract: Serotonin receptor 5-HT$_{2A}$ and tropomyosin receptor kinase B (TrkB) strongly contribute to neuroplasticity regulation and are implicated in numerous neuronal disorders. Here, we demonstrate a physical interaction between 5-HT$_{2A}$ and TrkB in vitro and in vivo using co-immunoprecipitation and biophysical and biochemical approaches. Heterodimerization decreased TrkB autophosphorylation, preventing its activation with agonist 7,8-DHF, even with low 5-HT$_{2A}$ receptor expression. A blockade of 5-HT$_{2A}$ receptor with the preferential antagonist ketanserin prevented the receptor-mediated downregulation of TrkB phosphorylation without restoring the TrkB response to its agonist 7,8-DHF in vitro. In adult mice, intraperitoneal ketanserin injection increased basal TrkB phosphorylation in the frontal cortex and hippocampus, which is in accordance with our findings demonstrating the prevalence of 5-HT$_{2A}$–TrkB heteroreceptor complexes in these brain regions. An expression analysis revealed strong developmental regulation of 5-HT$_{2A}$ and TrkB expressions in the cortex, hippocampus, and especially the striatum, demonstrating that the balance between TrkB and 5-HT$_{2A}$ may shift in certain brain regions during postnatal development. Our data reveal the functional role of 5-HT$_{2A}$–TrkB receptor heterodimerization and suggest that the regulated expression of 5-HT$_{2A}$ and TrkB is a molecular mechanism for the brain-region-specific modulation of TrkB functions during development and under pathophysiological conditions.

Keywords: tropomyosin receptor kinase B; 5-hydroxytryptamine 2A receptor; oligomerization; heteroreceptor; autophosphorylation

Citation: Ilchibaeva, T.; Tsybko, A.; Zeug, A.; Müller, F.E.; Guseva, D.; Bischoff, S.; Ponimaskin, E.; Naumenko, V. Serotonin Receptor 5-HT$_{2A}$ Regulates TrkB Receptor Function in Heteroreceptor Complexes. *Cells* **2022**, *11*, 2384. https://doi.org/10.3390/cells11152384

Academic Editor: Stefan Liebau

Received: 15 June 2022
Accepted: 29 July 2022
Published: 2 August 2022

1. Introduction

Tropomyosin receptor kinase B (TrkB) is a major transducer of intracellular signals from mature brain-derived neurotrophic factor (BDNF). TrkB is predominantly expressed within the CNS, especially in the frontal cortex, hippocampus, cerebellar cortex, visual system, hypothalamus, striatum, substantia nigra, and dorsal raphe nucleus [1–6]. The binding of BDNF to TrkB induces the autophosphorylation of tyrosine residues in the cytoplasmic domain of TrkB, resulting in the activation of the Ras–mitogen-activated protein kinase (MAPK), phosphoinositide 3-kinase (PI3K)–AKT, and phospholipase Cγ1 (PLC-γ1) signaling pathways [7,8]. BDNF–TrkB signaling plays important roles in the regulation of neuron survival and migration, neurite growth, and long-term potentiation [8–10]. Additionally, TrkB-mediated signaling is broadly recognized as a critical component of the responses to classic and unconventional antidepressants [11,12].

Serotonin receptor 2A (5-HT$_{2A}$) belongs to the G-protein-coupled receptor (GPCR) family and is broadly distributed within the brain, showing high expression in the olfactory

tubercle, cortical areas, and dentate gyrus [13,14]. Functionally, 5-HT_{2A} is involved in neurogenesis and can modulate synaptic plasticity via long-lasting increases in the excitability and firing rate of glutamatergic and GABAergic neurons [15,16]. The 5-HT_{2A} receptor is implicated in numerous CNS disorders, including bipolar disorder, depression, and schizophrenia [17,18]. A number of open-label and placebo-controlled clinical trials have revealed that some 5-HT_{2A}-blocking antipsychotic drugs elicit better clinical responses in bipolar or treatment-resistant depressive patients [19–24].

The coupling of 5-HT_{2A} with heterotrimeric G_q/G_{11} proteins results in the activation of phospholipase C (PLC), leading to increased Ca^{2+} release from the endoplasmic reticulum. In neurons, Ca^{2+} influx can activate cyclic AMP (cAMP) response element-binding protein (CREB), which, in turn, boosts the transcription of BDNF [25]. Interestingly, a number of studies show increased BDNF expression following 5-HT_{2A} stimulation [26–29], suggesting functional interplay between the 5-HT_{2A} and TrkB signaling pathways. Although the underlying mechanisms are not completely understood, a direct interaction between 5-HT_{2A} and TrkB may be an intriguing explanation. Research groups have demonstrated that 5-HT_{2A} can form heterodimers with other GPCRs, including the 5-HT_{1A} receptor [30], dopamine receptor D2 [31], and metabotropic glutamate receptor mGlu(2) [32]. Moreover, we have previously reported that other 5-HT receptors, including the 5-HT_4 and 5-HT_7 subtypes, can form heterodimers with adhesion molecule L1 [33], CDK5 [34], or CD44 [35], respectively. To date, no published data show that 5-HT_{2A} interacts with non-GPCR proteins.

In the present study, we found that 5-HT_{2A} and TrkB form heteroreceptor complexes both in vitro and in vivo. We further demonstrated the functional effects of 5-HT_{2A} and TrkB receptor heterodimerization.

2. Materials and Methods

2.1. Animals and Drugs

Adult (P60) male C57BL/6J mice (10–11 weeks old, 23–26 g, Jackson Laboratory, Bar Harbor, ME, USA, RRID:IMSR_JAX:000664) were used for acute treatment with ketanserin or 25CN-NBOH. The mice were housed under standard laboratory conditions in the natural light–dark cycle (16 h of light and 8 h of dark) with free access to water and food. The preferential 5-HT_{2A} antagonist ketanserin (Sigma Aldrich, St. Louis, MO, USA) or the selective 5-HT_{2A} agonist 25CN-NBOH (Tocris, Bristol, UK) was dissolved in saline, and each was administered i.p. at a dose of 1 mg/kg of body weight (eight mice in each group). The control group (eight mice) received an equivalent saline injection. At 10 min (for 25CN-NBOH) or 30 min (for ketanserin) after the injection, the animals were euthanized, the brains were removed on ice, and the frontal cortex, hippocampus, and striatum were dissected.

2.2. Cell Culture and Transfection

Mouse N1E-115 neuroblastoma cells from the American Type Culture Collection (ATCC, cat. # CRL-2263, RRID:CVCL_0451) were grown at 37 °C and 5% CO_2 in DMEM (Gibco, New York, NY, USA) that contained 10% of fetal bovine serum (Gibco, New York, NY, USA) and penicillin/streptomycin (100 U/mL, Gibco). Transient transfection was performed with Lipofectamine 2000 (Invitrogen) according to manufacturer's protocol, and after transfection cells were incubated in the serum-free medium. For treatments, we applied 500 nM selective TrkB agonist 7,8-DHF (Sigma Aldrich, St. Louis, MO, USA), 1 µM 25CN-NBOH (Tocris, Bristol, UK), and/or 1 µM ketanserin (Sigma Aldrich, St. Louis, MO, USA). The doses of all drugs were chosen based on literature data. In one work, it was shown that a 7,8-DHF concentration of 500 nM is maximally effective for TrkB activation [36]. 25CN-NBOH at 1 µM is highly selective for 5-HT_2 sites [37]. Ketanserin at 1 µM is known to block the 5-HT_{2A} receptor [38].

2.3. Recombinant-DNA Procedures

Murine 5-HT_{2A} cDNA was cloned into the pcDNA3.1(+) donor vector (Invitrogen, Carlsbad, CA, USA) carrying an HA-tag. TrkB_mEGFP was kindly gifted by Ryohei Yasuda

(Addgene plasmid # 83952; http://n2t.net/addgene:83952 (accessed on 13 July 2019); RRID: Addgene_83952).

2.4. Co-Immunoprecipitation

Co-immunoprecipitation in lysates of N1E-115 cells that co-expressed HA-tagged 5-HT_{2A} and GFP-tagged TrkB was performed as described previously [35] with an antibody against GFP (1:250; GeneTex, cat. # GTX26556, RRID:AB_371421). Immunoblotting was carried out using a horseradish peroxidase (HRP)-conjugated anti-GFP (1:1000; LSBio (LifeSpan, Providence, RI, USA), cat. # LS-C50850-500, RRID:AB_1220053) or an HRP-conjugated anti-HA tag (1:250; Roche, Basel, Switzerland, cat. # 12013819001, RRID:AB_390917) antibody.

Co-immunoprecipitation from hippocampal, cortical, and striatal homogenates was performed according to a protocol described elsewhere [39]. Briefly, brain samples isolated from adult (P90) C57BL/6J mice were homogenized, and membrane fractions were prepared by differential centrifugation. The lysates were incubated with a goat polyclonal antibody against 5-HT_{2A} (1:50; Santa Cruz Biotechnology, Dallas, TX, USA, cat. # sc-15073, RRID:AB_2119724) followed by incubation with Protein A-Sepharose and Western blotting with an anti-TrkB antibody (1:1000; R&D Systems, Minneapolis, MN, USA, cat. # AF1494, RRID:AB_2155264).

2.5. The Immunofluorescence Assay of Mouse Brain Sections

Adult (P90) male and female C57BL/6J mice were subjected to this assay. The mice were bred and housed at the animal facility of the University of Hohenheim at a controlled temperature (25 °C) and photoperiod (12/12 h light/dark cycle) and were allowed unrestricted access to standard food and tap water.

Mice were euthanized by CO_2 asphyxiation, the brains were removed, postfixed overnight at 4 °C, processed routinely, and embedded in paraffin. Next, 5 µm-thick sections were prepared on a Leica RM2255 microtome (Nussloch, Germany) and transferred to SuperFrost®Plus glass slides (Thermo Fisher Scientific, Waltham, MA, USA). The sections were air-dried at least overnight at 37 °C and then subjected to the immunofluorescence assay.

The brain sections were deparaffinized according to a standard protocol and washed with PBS. Antigen retrieval was performed by immersion in 0.01 M sodium citrate buffer (pH 9.0) heated at 80 °C in a water bath for 30 min. The blocking of nonspecific binding sites was performed for 1 h at room temperature in PBS containing 5% normal donkey serum (Jackson ImmunoResearch Laboratories, West Grove, PA, USA, cat. # 017-000-121), 0.1% Triton X-100 (Sigma-Aldrich, Darmstadt, Germany, cat. # 93427), and 0.02% sodium azide (Merck, Darmstadt, Germany). Incubation with rabbit polyclonal anti-5-HT_{2A} receptor (1:100, Abcam, Cambridge, UK, cat. # ab66049, RRID:AB_1141522) and goat polyclonal anti-TrkB (1:50, R&D Systems, cat. # AF1494, RRID:AB_2155264) antibodies diluted in PBS was carried out overnight at 4 °C. After a wash in PBS, appropriate secondary antibodies were applied for a 1 h incubation at room temperature: a donkey anti-rabbit IgG antibody conjugated with Alexa Fluor® 488 (Jackson ImmunoResearch Labs, RRID:AB_2313584, cat. # 711-545-152) and a donkey anti-goat IgG antibody conjugated with Alexa Fluor® 594 (Jackson ImmunoResearch Labs, RRID:AB_2340433, cat. # 705-585-147) both diluted 1:800 in PBS. After a subsequent wash in PBS, cell nuclei were visualized with a bis-benzimide solution (Hoechst 33,258 dye, 5 µg/mL in PBS; Sigma-Aldrich, St. Louis, MO, USA). Finally, the sections were mounted in an antiquenching medium and examined under a fluorescence microscope Zeiss Axiovert 200M (Zeiss, Göttingen, Germany) with 20× air objectives.

2.6. Linear Unmixing FRET Analysis

These measurements were performed on live N1E-115 neuroblastoma cells as described elsewhere [40]. 5-HT_{2A}-mTurquoise2 and TrkB-YPet served as the donor and acceptor, respectively. As a negative control, cells were co-transfected with mTurquoise2-tagged CD86 and YPet-tagged CD86. After 16 h, the cells were imaged with a Zeiss LSM 780 microscope equipped with a C-Apochromat 40×/1.2 W Korr water immersion objective

via the excitation of the fluorescent proteins at 440 and 514 nm according to the protocol. For the image analysis and evaluation, custom-written MATLAB scripts were employed. We calculated the predicted apparent FRET efficiency as $Ef_{DA} = \frac{1}{2} Ef_D/(1 - x_D) = \frac{1}{2} Ef_A/x_D$, assuming a standard dimerization model [39,41].

2.7. Analysis of Ca^{2+} Activity

This assay was performed on N1E-115 cells expressing TrkB-YPet, 5-HT_{2A}-mTurquoise2, or both. We acquired time series data under the Zeiss LSM 780 microscope for 10 min per recording (5 s per frame). Ca^{2+} activity was assessed by means of GCaMP6f fluorescence signals (F) and changes calculated as F/F_{max}. To raise Ca^{2+} levels to saturated, 10 µM ionomycin was applied after 6 min. This saturated Ca^{2+} signal was used as F_{max} for the calculation of basal Ca^{2+} levels.

2.8. In Situ Proximity Ligation Assay (PLA)

A PLA assay was performed with the Duolink in situ PLA Probes and Duolink in situ Detection Reagents Red Kit (cat. # DUO92008). Brain sections of 20 µm thickness were utilized in the PLA. Antibodies, the same as those used for immunohistochemistry, were diluted 1:100 with the Antibody Diluent provided with the kit. For imaging, the slides were dried and mounted with a cover slip by means of ~7 µL of the Duolink in situ Mounting Medium with 4′,6-diamidino-2-phenylindole (DAPI). The imaging and analysis of the stained brain sections were carried out under the fluorescence confocal microscope (Zeiss LSM 780) using a 40× objective and excitation wavelengths of 561 nm for PLA and 405 nm for DAPI. In each brain section, 3–4 measurements in the frontal cortex, hippocampus, and striatum were performed. Each image was analyzed in ImageJ (Fiji, RRID:SCR_002285) to count individual fluorescent spots. The data are presented as the number of spots per cell, normalized to the number of cells.

2.9. qRT-PCR

Total RNA was extracted from the brain tissue of C57BL/6J mice using ExtractRNA (Evrogen, Moscow, Russia), treated with RNA-free DNase (Promega, Madison, WI, USA), and diluted to 0.125 µg/µL with diethyl pyrocarbonate-treated water. One microgram of total RNA was subjected to cDNA synthesis with a random hexanucleotide mixture [42–44]. The number of cDNA copies for all studied genes was evaluated by qPCR on a LightCycler 480 (Roche Applied Science, Rotkreuz, Switzerland) with specific primers (Table 1), SYBR Green I fluorescence detection (R-414 Master mix, Syntol, Moscow, Russia), and 50, 100, 200, 400, 800, 1600, 3200, or 6400 copies of genomic DNA as external standards. The calibration curve in the coordinates Ct (threshold cycle value) and minus log P (decimal logarithm of the amount of DNA standard) was plotted automatically using the LightCycler 480 System software. Gene expression is presented as the relative number of cDNA copies per 100 copies of DNA-dependent RNA polymerase 2 subunit A (*Polr2a*) cDNA, which served as an internal standard [42–44]. A melting-curve analysis was performed at the end of each run for each primer pair, allowing us to control the amplification specificity.

Table 1. The primer sequences, annealing temperatures, and PCR products' lengths.

Target Gene	Primer Sequences	Annealing Temperature, °C	Amplicon Length, bp
Ntrk2	F 5′-cattcactgtgagaggcaacc-3′ R 5′-atcagggtgtagtctccgttatt-3′	63	175
Htr2a	F 5′-agaagccaccttgtgtgtga-3′ R 5′-ttgctcattgctgatggact-3′	61	169
Polr2a	F 5′-gttgtcgggcagcagaatgtag-3′ R 5′-tcaatgagaccttctcgtcctcc-3′	63	188

2.10. Western Blotting

The extraction of total protein from N1E-115 cells was performed in RIPA buffer (150 mM NaCl, 1.0% IGEPAL CA-630, 0.5% sodium deoxycholate, 0.1% SDS, and 50 mM Tris-HCl, pH 8.0) with the addition of 1 mM Na_3VO_4, 2 mM phenylmethylsulfonyl fluoride, and a protease and phosphatase inhibitor cocktail. The protein concentration was estimated spectrophotometrically using the Pierce BCA Protein Assay Kit (Thermo Fisher Scientific Inc., Waltham, MA, USA) and a NanoDrop 2000C spectrophotometer (Thermo Scientific, Waltham, MA, USA), followed by the adjustment of samples to equal concentrations with 2× Laemmli sample buffer. After denaturation by boiling for 10 min at 95 °C, the cell extracts (10 µg of total protein per lane) were resolved on 10% SDS-PAGE and blotted onto a nitrocellulose membrane (Bio-Rad Laboratories, Hercules, CA, USA). The membrane was incubated with a primary antibody (an anti-TrkB (1:1000; R&D Systems, cat. # AF1494, RRID:AB_2155264), anti-pTrkB (1:1000; Abcam, cat. # ab51187, RRID:AB_874043), or anti-5-HT_{2A} antibody (1:300; Abcam, cat. # ab66049, RRID:AB_1141522)) at 4 °C overnight, then the membrane was washed in Tris-buffered saline supplemented with 0.05% Tween 20 (TBS-T) and incubated with an HRP-conjugated secondary antibody. After protein detection, the blot was stripped and then re-probed with an anti-β-tubulin antibody (1:20,000; Abcam, cat. # ab6046, RRID:AB_2210370) as a loading control. Immunoreactive bands were detected by means of the Clarity Western ECL Substrate (Bio-Rad Laboratories, Hercules, CA, USA). Protein bands were documented on a C-DiGit Blot Scanner (LI-COR, Lincoln, NE, USA) and quantified in the Image Studio software (LI-COR Image Studio Software, RRID:SCR_015795, Lincoln, NE, USA). Target protein levels were assessed in chemiluminescence relative units and normalized to β-tubulin chemiluminescence relative units.

2.11. Statistical Analysis

The data are presented as means ± the standard error of the mean (SEM). Unless stated otherwise, the significance of pairwise differences was assessed by Student's *t* test after a Gaussian distribution evaluation by the D'Agostino–Pearson normality test. Groupwise comparisons were made by one-way ANOVA followed by Fisher's post hoc test. Cell groups co-expressing different amounts of 5-HT_{2A} receptors and treated with 7,8-DHF were compared by two-way ANOVA followed by Fisher's post hoc test. In figures, significance is displayed as $p < 0.05$ (*), $p < 0.01$ (**), and/or $p < 0.001$ (***).

3. Results

3.1. 5-HT_{2A} and TrkB Receptors Form Heterodimers in Neuroblastoma N1E-115 Cells

To analyze the specific interaction between 5-HT_{2A} and TrkB, we performed co-immunoprecipitation experiments with neuroblastoma N1E-115 cells co-expressing HA-tagged 5-HT_{2A} and GFP-tagged TrkB. It is noteworthy that non-transfected N1E-115 cells express neither 5-HT_{2A} nor TrkB (data not shown). After immunoprecipitation with an antibody against the HA tag, GFP-tagged TrkB was detectable only in cells co-expressing both HA- and GFP-tagged receptors (Figure 1A). To assay the extent of artificial protein aggregation, cells expressing only one receptor type (either HA-5-HT_{2A} or GFP-TrkB) were mixed prior to lysis and analyzed in parallel. While individual receptors could be detected by the same antibody, co-immunoprecipitation did not occur (Figure 1A). This result confirmed the specificity of the 5-HT_{2A}–TrkB hetero-oligomerization.

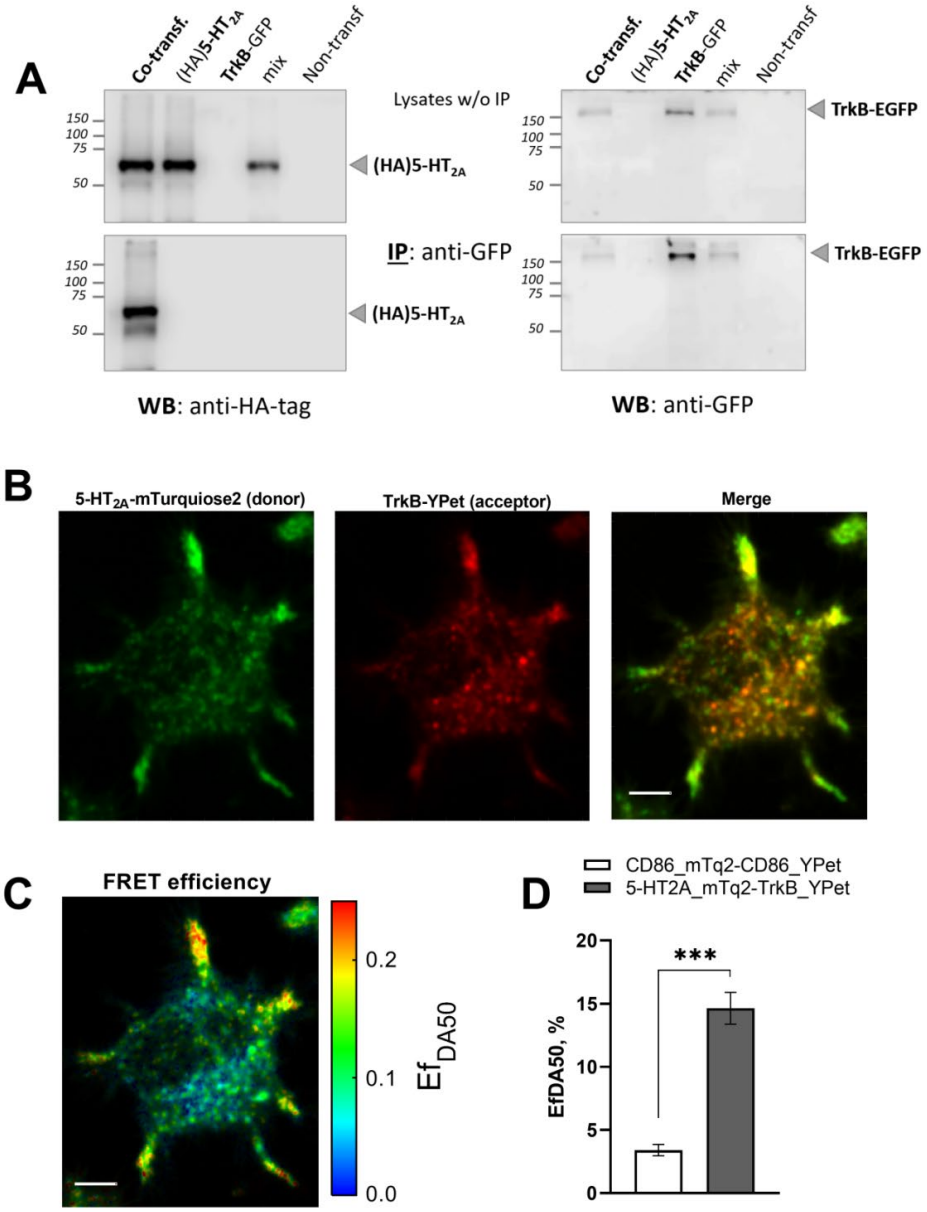

Figure 1. Interaction between receptors 5-HT_{2A} and TrkB in neuroblastoma N1E-115 cells. (**A**) Co-immunoprecipitation of recombinant HA-tagged 5-HT_{2A} and GFP (mEGFP)-tagged TrkB. Using a mixture of cells expressing each individual protein (mix) or cells that co-expressed both proteins (co-transfection), we performed immunoprecipitation (IP) with an anti-GFP antibody, followed by Western blot (WB) analysis with anti-GFP (right) and anti-HA (left) antibodies. Top: Expression of proteins before IP (lysate w/o IP). Bottom: Expression of proteins after IP. Results are representative of at least three independent experiments. (**B**–**D**) Specific interaction between 5-HT_{2A}-mTurquoise2 and TrkB-YPet. Cells co-expressing 5-HT_{2A}-mTurquoise2 and TrkB-YPet were analyzed using the lux-FRET method after confocal microscopy. (**B**) Distributions of 5-HT_{2A}-mTurquoise2 (donor) and TrkB-YPet (acceptor), and merged images quantified by linear unmixing of the fluorescence emission spectra. Scale bar, 5 µm. (**C**) Apparent FRET efficiency (Ef_{DA}). A representative cell is shown. (**D**) Quantification of FRET efficiency (Ef_{DA}) between 5-HT_{2A}-mTurquoise2 and TrkB-YPet. *** $p < 0.001$ (one-way ANOVA).

To overcome the limitations related to protein solubilization and concentration during the co-immunoprecipitation procedure, which can cause artificial protein aggregation [45], we further analyzed the interaction between 5-HT_{2A} and TrkB in living cells using a Förster resonance energy transfer (FRET)-based approach. We measured the apparent FRET

efficiency (Ef_{DA}) between mTurquoise2-labeled 5-HT_{2A} (5-HT_{2A}-mTurquoise2, donor) and YPet-labeled TrkB (TrkB-YPet, acceptor) in living N1E-115 cells using the linear unmixing FRET (lux-FRET) method combined with confocal microscopy (Figure 1B–D). This approach can detect the physical interaction of individual molecules on the nanoscale [40]. The lux-FRET analysis revealed a high apparent FRET efficiency (Ef_{DA} = 14.6%) for 5-HT_{2A}-mTurquoise2 and TrkB-YPet. In contrast, cells expressing a monomeric fluorophore-tagged CD86 protein [46] yielded significantly lower Ef_{DA} values (Figure 1D). These experiments demonstrated the selective heterodimerization of 5-HT_{2A} and TrkB.

3.2. Endogenous 5-HT_{2A} and TrkB Receptors Form a Protein Complex in the Mouse Brain

Having identified the interaction between recombinant 5-HT_{2A} and TrkB receptors in vitro, we next investigated whether this interaction also occurs in vivo. An immunohistochemical analysis was performed on slices of mouse hippocampus, cortex, and striatum, revealing that 5-HT_{2A} and TrkB receptors were highly co-localized (Figure 2A). We then performed a co-immunoprecipitation assay using brain tissue lysates from C57BL/6J mice and identified 5-HT_{2A}–TrkB oligomeric complexes in samples from the frontal cortex, hippocampus, and striatum (Figure 2B).

As an additional highly sensitive assay of hetero-oligomerization, we performed an in situ proximity ligation assay (PLA) [47]. In all analyzed brain regions (striatum, hippocampus, and cortex), we found specific PLA-positive blobs, confirming the physical interaction between 5-HT_{2A} and TrkB (Figure 2C). The quantification revealed a significantly higher number of 5-HT_{2A}–TrkB heterodimers in hippocampal cells, indicating a greater prevalence of 5-HT_{2A}–TrkB heteromeric complexes in this brain region compared to in the frontal cortex and striatum (Figure 2D).

3.3. Calcium Signaling Is Not Affected by the Heterodimerization

To evaluate possible functional consequences of TrkB–5-HT_{2A} heterodimerization, we first assessed Ca^{2+} activity in N1E-115 cells expressing TrkB-YPet, 5-HT_{2A}-mTurquoise2, or both. To this end, we used the Ca^{2+} indicator GCaMP6f [48] and analyzed Ca^{2+} dynamics with the multi-threshold event detection approach [49]. The ratio of the GCaMP6f fluorescent signal (F) to the saturated Ca^{2+} signal (F_{max}) indicated that basal Ca^{2+} levels were significantly higher following heterodimerization compared to control cells (Figure 3). The addition of the Ca^{2+} ionophore ionomycin to N1E-115 cells elevated Ca^{2+} levels under all conditions, with a significantly stronger signal in cells expressing either 5-HT_{2A} alone or co-expressing TrkB and 5-HT_{2A} (Figure 3). This finding may reflect constitutive 5-HT_{2A} activity [50–52]. On the other hand, the basal Ca^{2+} levels did not differ between cells expressing 5-HT_{2A} and those co-expressing TrkB and 5-HT_{2A} (Figure 3), indicating that 5-HT_{2A}–TrkB hetero-oligomerization did not affect the constitutive 5-HT_{2A} receptor activity toward a Ca^{2+} response. Based on this observation, we focused on whether heterodimerization had functional consequences for TrkB receptors.

3.4. Heterodimerization Reduces TrkB Phosphorylation and Blunts the Response to 7,8-DHF

The dimerization and autophosphorylation of tyrosine residues in the intracellular kinase domain of TrkB are crucial steps for the activation of TrkB-mediated intracellular signaling cascades [8]. To determine whether 5-HT_{2A}–TrkB heterodimerization led to changes in TrkB phosphorylation, we examined the level of the phosphorylated TrkB (pTrkB) protein in N1E-115 cells, using a phospho-specific antibody that specifically recognizes the Y515 site [53]. Notably, the basal pTrkB/TrkB ratio was significantly reduced in cells co-expressing 5-HT_{2A} (Figure 4). Moreover, 5-HT_{2A} co-expression not only decreased the amount of phosphorylated TrkB but also prevented its activation by 7,8-DHF, a well-known high-affinity TrkB agonist (Figure 4A) [36,54]. We also treated cells co-expressing 5-HT_{2A} and TrkB with the selective 5-HT_{2A} receptor agonist 25CN-NBOH, which had no significant impact on the pTrkB/TrkB ratio (Figure 4B).

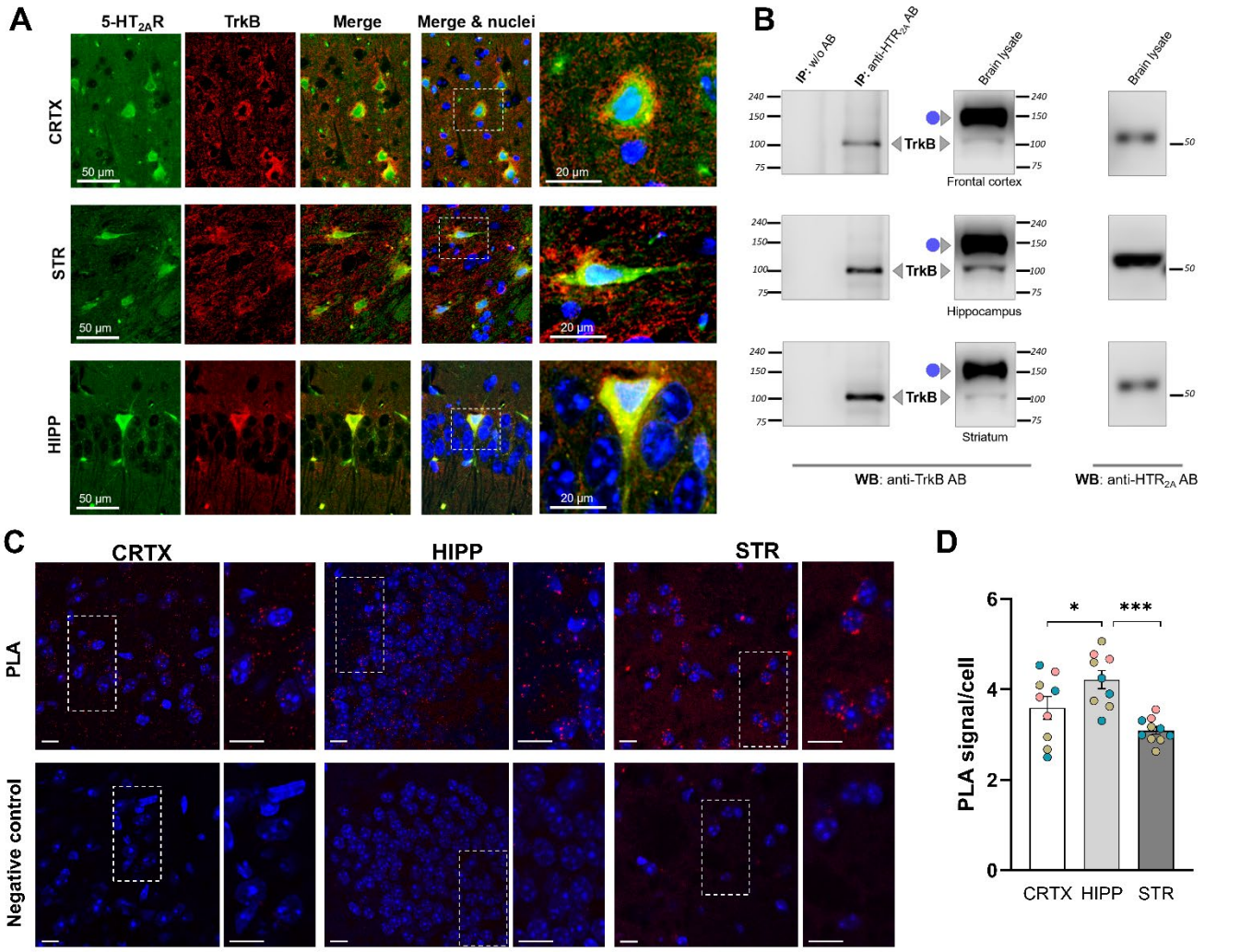

Figure 2. Interaction between receptors 5-HT_{2A} and TrkB in the mouse brain. (**A**) Co-localization of 5-HT_{2A} and TrkB in the mouse brain. Brain slices from cortex (CRTX), striatum (STR), and hippocampus (HIPP) were subjected to immunohistochemistry for the detection of 5-HT_{2A} (green) and TrkB (red), followed by confocal microscopy. Nuclei are shown in blue. Right: Merged images and a magnified view of representative neurons. (**B**) Co-immunoprecipitation between 5-HT_{2A} and TrkB in brain lysates. Whole-brain homogenates were prepared from different brain areas and subjected to IP with an anti-5-HT_{2A} receptor antibody, followed by WB analysis with anti-TrkB and anti-5-HT_{2A} antibodies. AB: antibody; IP, immunoprecipitation; WB, Western blot; • glycosylated TrkB. Results are representative of at least three independent experiments. (**C**) Detection of 5-HT_{2A}–TrkB heteroreceptor complexes in mouse brain slices using proximity ligation assay (PLA). Representative images of PLA staining in cortex (CRTX), hippocampus (HIPP), and striatum (STR) are shown as a single Z-stack. Nuclei are shown in blue, and PLA blobs are shown in red. Negative control was performed omitting primary antibodies. Scale bar, 20 µm. (**D**) Quantification of the 5-HT_{2A}-TrkB heterodimer density. Data are presented as means ± SEM (n = 6 mice). Each colored dot represents data obtained for one mouse. * $p < 0.05$, *** $p < 0.001$ (one-way ANOVA).

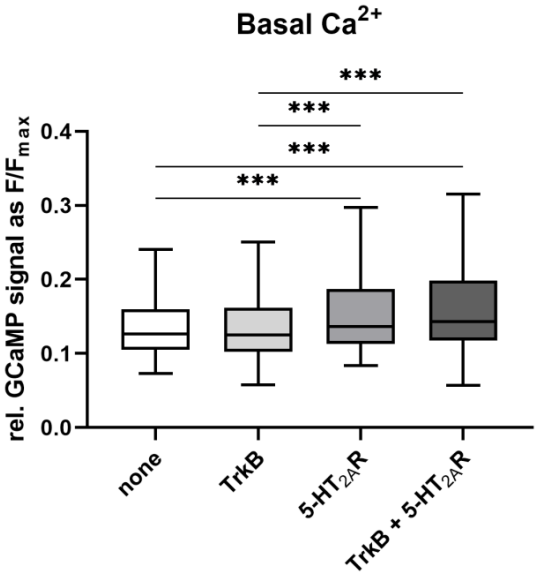

Figure 3. Heterodimerization does not affect basal Ca^{2+} levels in N1E-115 cells. Neuroblastoma cells were transfected with Ca^{2+} indicator GCaMP6f, either alone or together with 5-HT_{2A}-mTurquoise2, TrkB-YPet, or both. Basal Ca^{2+} activity was calculated as F/F_{max}. To saturate Ca^{2+} levels, 10 µM ionomycin was applied after 6 min of recording. The saturated Ca^{2+} signal was used as F_{max}. Data are presented as means ± SEM ($12 \leq n \leq 17$). *** $p < 0.001$ (Kruskal–Wallis test with Dunn's multiple-comparison post hoc test).

We then tested whether the heterodimerization rate influenced TrkB phosphorylation. To this end, we analyzed cells expressing a constant amount of TrkB (1 µg), either alone or together with an increasing concentration of HA-tagged 5-HT_{2A} (Figure 4C). Basal TrkB phosphorylation was significantly reduced by the expression of even a small amount (0.25 µg) of 5-HT_{2A} receptor. Treatment with 7,8-DHF yielded a robust enhancement of TrkB phosphorylation in cells expressing TrkB alone, and this response continuously diminished when TrkB was co-expressed with increasing amounts of 5-HT_{2A} (Figure 4B).

3.5. Expression Patterns of TrkB and 5-HT_{2A} during Postnatal Development

The results depicted in Figure 4 suggest that 5-HT_{2A}–TrkB oligomerization impacted TrkB function in a manner depending on the receptors' expression ratio. Therefore, we next determined the expression profiles of 5-HT_{2A} and TrkB in mouse hippocampus, striatum, and cortex at different stages of postnatal development using real-time quantitative RT-PCR. An analysis of the Ntrk2 transcript encoding TrkB revealed that the Ntrk2 mRNA level was continuously elevated from P1 to P30 in the hippocampus and frontal cortex and that this increase was sustained in the striatum until P60 (Figure 5B).

An analysis of the *Htr2a* gene transcript encoding 5-HT_{2A} revealed that the mRNA level continuously increased from P1 to P60 in the hippocampus and cortex but not in the striatum (Figure 5A). Moreover, the number of *Ntrk2* transcripts was approximately 10 times higher than that of *Htr2a* transcripts (Figure 5A). In the hippocampus and cortex, the *Htr2a*/*Ntrk2* mRNA ratio mimicked the pattern of mRNA levels, while the *Htr2a*/*Ntrk2* mRNA ratio in the striatum drastically increased from P1 to P60 (Figure 5C). These findings suggest that the balance between TrkB and 5-HT_{2A} may shift in certain brain regions during postnatal development. In light of the above-described suppressive effects of 5-HT_{2A} on TrkB phosphorylation, this balance might significantly impact TrkB functions. Considering that the physiological ratio of 5-HT_{2A} to TrkB does not exceed 0.2, we examined TrkB phosphorylation in N1E-115 cells expressing a constant amount of TrkB with near-physiological (0.01–0.25 µg) concentrations of HA-tagged 5-HT_{2A}. These experiments revealed significantly reduced basal phosphorylation of TrkB in the cells expressing 5-HT_{2A} at concentrations ≥0.05 µg (Figure 5D).

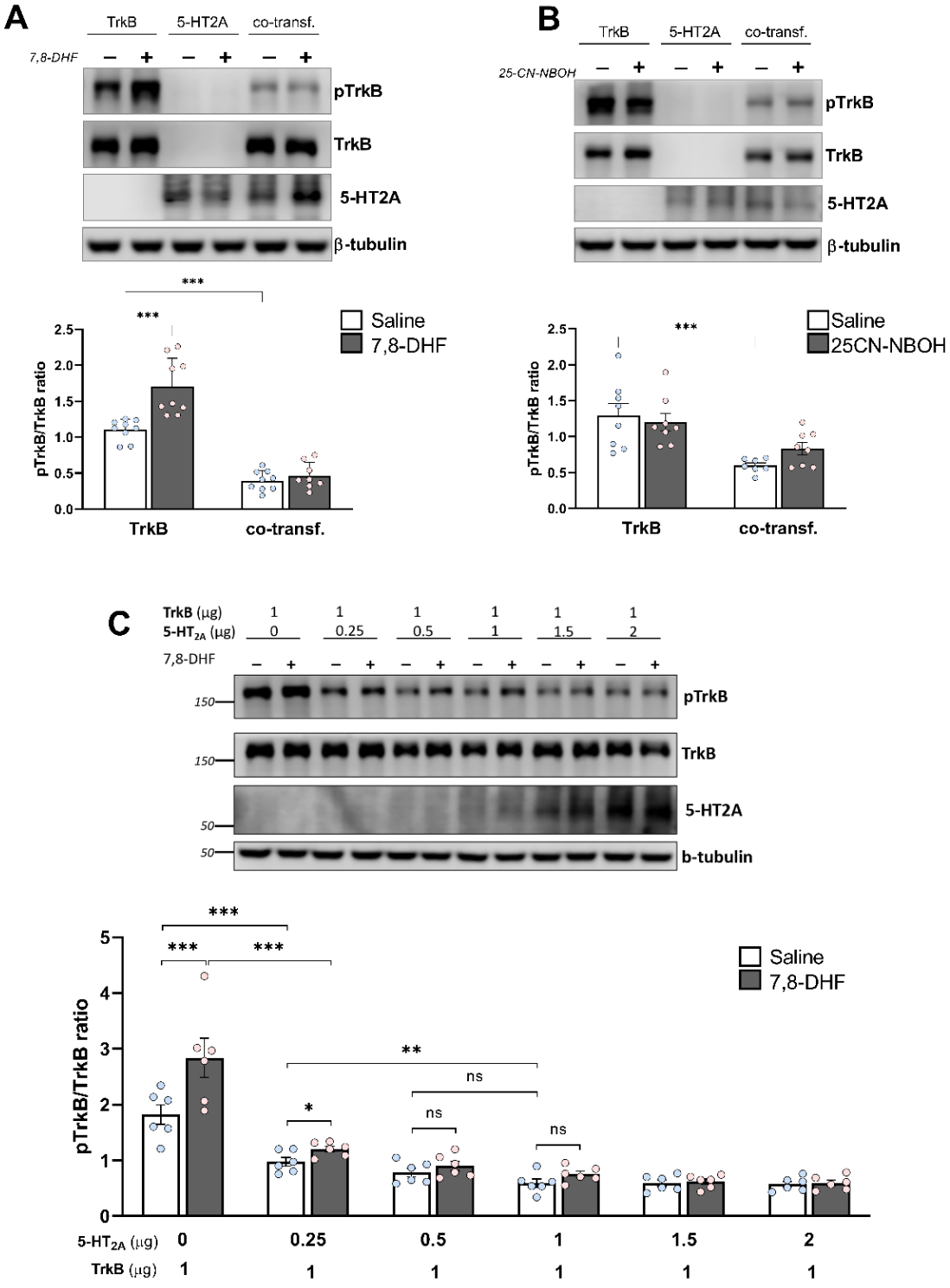

Figure 4. Heterodimerization affects TrkB phosphorylation. (**A**,**B**) Analysis of TrkB phosphorylation. Neuroblastoma N1E-115 cells expressing either HA-tagged 5-HT_{2A} (1 μg), GFP-tagged TrkB (1 μg), or co-expressing equal amounts of both receptors were treated for 30 min with either (**A**) the 5-HT_{2A} receptor agonist 25CN-NBOH (1 μM) or (**B**) the TrkB agonist 7,8-DHF (500 nM). Cells were lysed, followed by SDS-PAGE and Western blot (WB) analysis using antibodies against either total TrkB or phosphorylated TrkB. The 5-HT_{2A} receptor was detected in parallel. In WB, ß-tubulin was used as a loading control. Representative Western blots are shown. Lower panels show the quantification of TrkB phosphorylation, which was performed by densitometry and calculated as the ratio of total TrkB

expression to the TrkB phosphorylation signal after adjustment for the general expression level. Bars show means ± SEM ($n \leq 8$). *** $p < 0.001$ (two-way ANOVA). (**C**) Heterodimerization affects agonist-mediated TrkB phosphorylation. Neuroblastoma cells were co-transfected with 1 µg of cDNA encoding the GFP-tagged TrkB receptor, together with increasing concentrations of HA-tagged 5-HT_{2A} receptor. Cells were treated for 30 min with either 500 nM 7,8-DHF or vehicle, followed by WB analysis. Lower panel: Quantification of TrkB phosphorylation. Bars show means ± SEM ($n = 6$). ns: not significant, * $p < 0.05$, ** $p < 0.01$, *** $p < 0.001$ (two-way ANOVA).

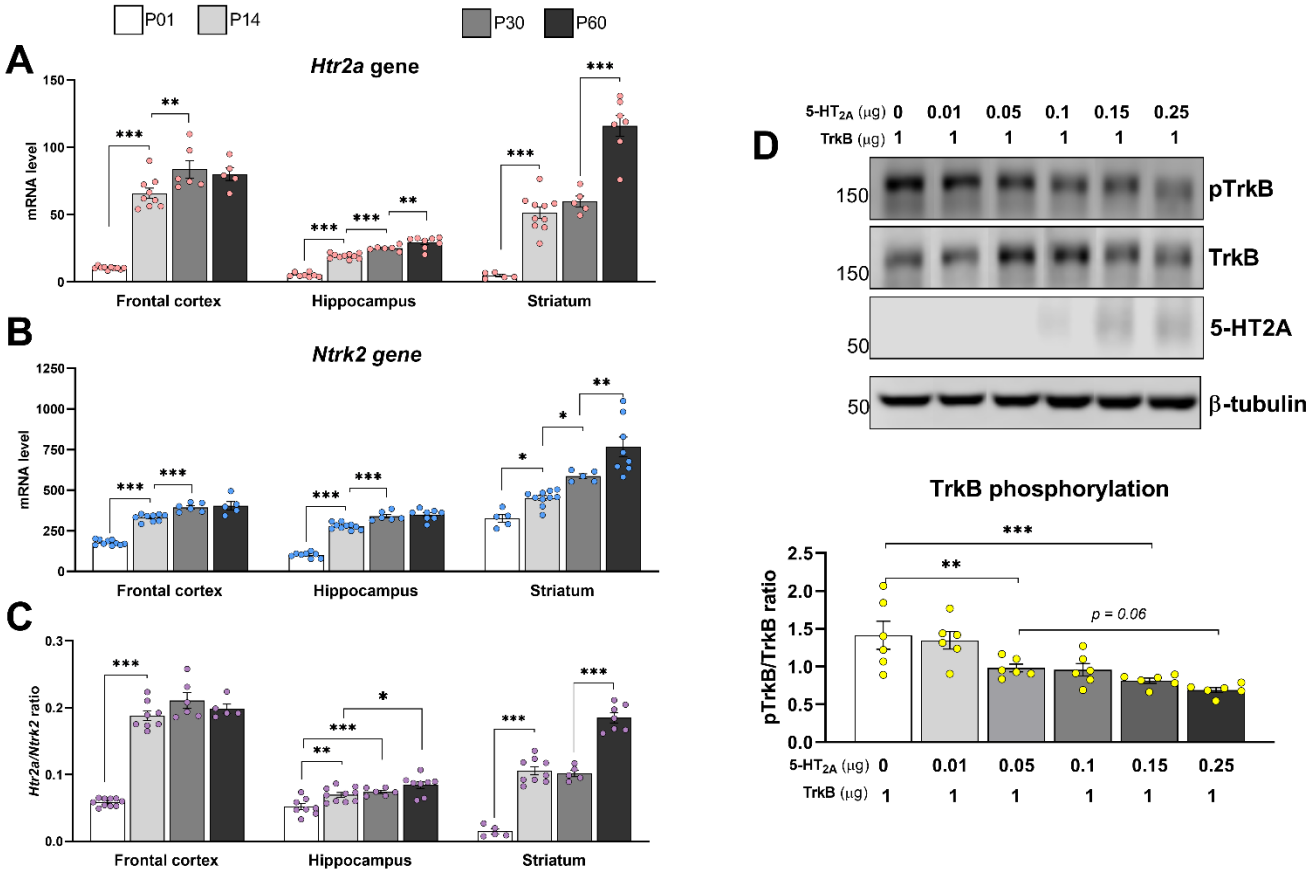

Figure 5. Expression profiles of TrkB and 5-HT_{2A} receptors during postnatal development. (**A**,**B**) Expression levels of mRNAs encoding 5-HT_{2A} (**A**) and TrkB (**B**) in the indicated brain regions were determined at different stages of postnatal development using real-time PCR. Gene expression is presented as the number of gene cDNA copies per 100 cDNA copies of *Polr2a*, used as a calibration control. (**C**) Expression ratios between 5-HT_{2A} and TrkB. Bars represent means ± SEM ($5 \leq n \leq 10$). * $p < 0.05$; ** $p < 0.01$ *** $p < 0.001$ (one-way ANOVA). (**D**) Heterodimerization exerts an inhibitory effect on agonist-independent TrkB autophosphorylation. Neuroblastoma cells were co-transfected with 1 µg of cDNA encoding the GFP-tagged TrkB receptor, together with increasing concentrations of HA-tagged 5-HT_{2A} receptor, followed by Western blot (WB) analysis. Lower panel: Quantification of TrkB phosphorylation. Bars show means ± SEM ($n = 6$). ns: not significant, $p = 0.06$: an insignificant trend; ** $p < 0.01$, *** $p < 0.001$ (one-way ANOVA).

3.6. Restoration of TrkB Phosphorylation by Ketanserin Treatment

We next analyzed whether a pharmacological 5-HT_{2A} receptor blockade could restore TrkB phosphorylation. To address this question, we pretreated N1E-115 cells expressing both receptors with the preferential 5-HT_{2A} antagonist ketanserin. It is noteworthy that after ketanserin treatment basal TrkB autophosphorylation was recovered to the level obtained in the cells expressing TrkB alone. In contrast, the 5-HT_{2A} receptor blockade by ketanserin did not restore the TrkB phosphorylation in response to 7,8-DHF treatment (Figure 6A).

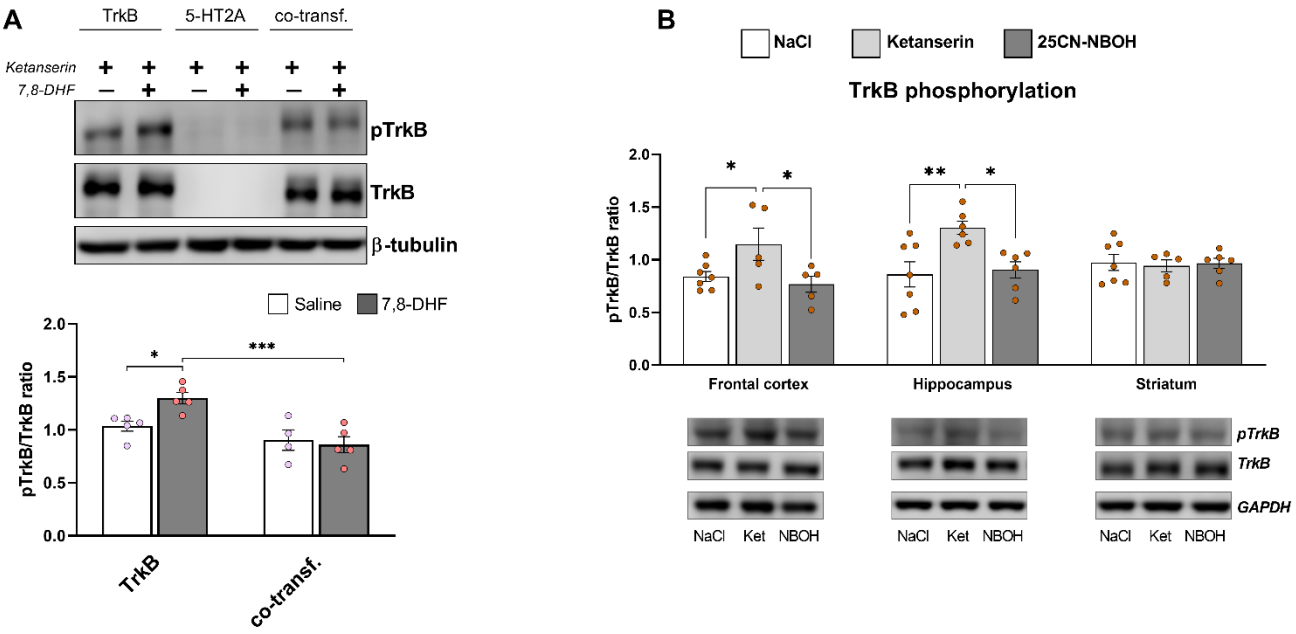

Figure 6. Blockade of 5-HT_{2A} with ketanserin reversed TrkB autophosphorylation in vitro and in vivo. (**A**) Neuroblastoma N1E-115 cells expressing HA-tagged 5-HT_{2A} receptor, GFP-tagged TrkB, or co-expressing both receptors were treated with the 5-HT_{2A} receptor antagonist ketanserin (1 μM) for 10 min, followed by treatment with either 7,8-DHF (500 nM) or vehicle for 30 min. Cell lysates were then subjected to SDS-PAGE and Western blot (WB) analysis with antibodies against phosphorylated or total TrkB. β-tubulin was used as a loading control. Representative WBs are shown. Bars show means ± SEM ($n \leq 8$). * $p < 0.05$; *** $p < 0.001$ (two-way ANOVA). (**B**) Mice were intraperitoneally injected with ketanserin (1 mg/kg) or 25CN-NBOH (1 mg/kg), resulting in increased TrkB phosphorylation in the hippocampus and frontal cortex. At 10 min (for 25CN-NBOH) or 30 min (for ketanserin) after injection, the animals were euthanized, and brain lysates were prepared from the frontal cortex, hippocampus, and striatum. This was followed by SDS-PAGE and WB to detect phosphorylated and total TrkB. GAPDH was used as a loading control. Representative WBs are shown. Bars represent means ± SEM ($5 \leq n \leq 8$) * $p < 0.05$; ** $p < 0.01$ (two-way ANOVA).

To determine whether 5-HT_{2A} blockade or activation could alter TrkB autophosphorylation in vivo, we intraperitoneally injected adult (P60) C57BL/6J mice with either ketanserin (1 mg/kg) or the selective 5-HT_{2A} agonist 25CN-NBOH (1 mg/kg). TrkB phosphorylation was significantly increased in the hippocampus and frontal cortex of mice treated with ketanserin but not those treated with 25CN-NBOH (Figure 6B).

These results implied that 5-HT_{2A}–TrkB heterodimerization specifically attenuates TrkB autophosphorylation and that the heterodimerization rate specifically regulates agonist-mediated TrkB phosphorylation. In vitro 5-HT_{2A} blockade with the selective antagonist ketanserin reversed the decrease of basal TrkB autophosphorylation but failed to restore the TrkB response to 7,8-DHF. At the same time, ketanserin administration considerably enhanced TrkB phosphorylation in the mouse brain in vivo.

4. Discussion

Several research articles have reported the modulation of BDNF expression by the 5-HT_{2A} receptor within the limbic neurocircuits [27–29], but the exact underlying mechanisms remain unclear. Moreover, the TrkB receptor can be involved in 5-HT_{2A}-mediated neurito- and spinogenesis in cortical neuronal cultures [55]. We recently found that the chronic treatment of mice with the selective 5-HT_{2A} receptor agonists TCB-2 and 25CN-NBOH reduced the levels of total and membrane-associated TrkB protein in the mouse brain [56], indicating TrkB downregulation. Among several possible explanations for the functional interplay

between 5-HT_{2A} and TrkB, heterodimerization is the most intriguing. Previously, we have reported that the 5-HT_4 or 5-HT_7 receptors, the classical GPCRs, can form heterodimers with adhesion molecule L1 [33], CDK5 [34], or CD44 [35]. The existence of heteroreceptor complexes between GPCRs and receptor tyrosine kinases (RTKs) was demonstrated previously for the adenosine receptor A2AR [57,58]. Moreover, the 5-HT_{1A} receptor has previously been shown to form heteroreceptor complexes with fibroblast growth factor receptor 1 (FGFR1) in the mouse hippocampus [59]. In the present study, we used a combination of multiple approaches (including lux-FRET, PLA, and co-immunoprecipitation) to demonstrate the existence of 5-HT_{2A}-TrkB heteroreceptor complexes both in vitro and in vivo.

From a functional perspective, this heterodimerization suppressed basal TrkB autophosphorylation and prevented agonist-mediated TrkB activation without affecting 5-HT_{2A} receptor functions. Importantly, our data demonstrated that the degree of heterodimerization played a pivotal role in this process. This suggests that changes in the relative amounts of both receptors and the corresponding changes in heterodimerization rates can provide an intriguing mechanism for the differential regulation of TrkB functions in health and disease. Several studies have described substantially decreased TrkB expression and lower TrkB phosphorylation in the hippocampus of depressive suicidal victims [60–63]. There is also evidence of increased 5-HT_{2A} levels in some brain structures, including the frontal cortex and hippocampus, in post-mortem samples from patients with major depressive disorder and suicide victims [64–66]. Moreover, 5-HT_{2A} expression is reportedly sensitive to basal 5-HT concentration, with the 5-HT_{2A} receptor becoming more abundant in response to a diminished synaptic 5-HT concentration and vice versa [67–69]. In this regard, the general tendency of upregulated 5-HT_{2A} expression in the brain of suicide victims may be explained by an adaptive response to deficient 5-HT_{2A} signaling due to a reduced 5-HT level in depression. Based on the above-mentioned data, it might be hypothesized that under pathological conditions (e.g., major depressive disorder, addiction, and suicidal behavior), the balance between 5-HT_{2A} and TrkB becomes shifted toward increased levels of 5-HT_{2A}–TrkB heteroreceptor complexes, with a subsequent loss of TrkB function. The prevalence of 5-HT_{2A}–TrkB heteroreceptor complexes in the hippocampus, even under the basal conditions obtained in this study, suggests that this brain structure is among the most vulnerable to the above scenario.

Notably, our findings may also explain why the ability of BDNF to activate TrkB gradually declines during early postnatal development in mice [70]. Starting from approximately 2 weeks of age, BDNF application has only a weak influence on TrkB phosphorylation, while the systemic administration of selective serotonin reuptake inhibitors begins to affect TrkB signaling. Here, we showed that at P14 5-HT_{2A} expression was drastically increased (up to five-fold) in all analyzed brain regions, while TrkB expression exhibited only a moderate change (up to a two-fold increase). Considering that even a very low relative amount of 5-HT_{2A} receptor elicited inhibitory effects on TrkB, such a shift in the receptor ratio could result in the decreased ability of BDNF to activate TrkB.

The 5-HT_{2A}–TrkB interaction could also play a role in the action of antidepressants. It is generally accepted that BDNF–TrkB signaling is a critical component of an antidepressant response [11,71–73]. On the other hand, accumulating evidence from animal and clinical studies suggests that 5-HT_{2A} receptor inactivation may also facilitate antidepressant action [23,74–77]. In one study, chronic treatment with a relatively high dosage (5 mg/kg) of the 5-HT_{2A} receptor antagonist ketanserin increased neurogenesis in the adult rat hippocampus [78]. However, this effect might be unspecific to the 5-HT_{2A} receptors because a combined treatment with fluoxetine and ketanserin applied at lower dosage (i.e., 0.1 mg/kg) failed to produce a neurogenic effect while it boosted the expression of *Bdnf* mRNA in the rat hippocampus [79]. Moreover, atypical antipsychotics exerting 5-HT_{2A} antagonism can stimulate BDNF expression and/or secretion [80–90]. On the other hand, 5-HT_{2A} receptor activation can suppress *Bdnf* transcription in the hippocampus [26]. Our present data showing the physical interaction of 5-HT_{2A} and BDNF could thus explain the

functional crosstalk between these receptors at the molecular level. Indeed, we found that an acute blockade of 5-HT_{2A} with ketanserin reversed basal TrkB phosphorylation in vitro. We also demonstrated that acute treatment with ketanserin led to increased TrkB phosphorylation in the mouse hippocampus and frontal cortex in vivo, which is in accordance with our findings regarding the prevalence of 5-HT_{2A}–TrkB heteroreceptor complexes in these brain regions.

Overall, our present results demonstrated that the 5-HT_{2A} receptor, a member of the GPCR family, could form heterodimers with the non-GPCR receptor TrkB, both in vitro and in vivo. Heterodimerization considerably decreased TrkB autophosphorylation and prevented TrkB activation by its ligand, and these effects could be reversed by a pharmacological blockade of 5-HT_{2A} with ketanserin. Importantly, our findings suggest that the regulated and balanced ratio of heterodimerization in different brain structures may be crucially involved in both the onset and treatment responsiveness of psychiatric diseases such as depression and anxiety.

5. Conclusions

In the present study, we provide a multilevel analysis demonstrating, for the first time, the physical interaction between the 5-HT_{2A} receptor, a member of the GPCR family, and the non-GPCR receptor TrkB, both in vitro and in vivo.

From a functional perspective, heterodimerization suppressed basal TrkB autophosphorylation and prevented agonist-mediated TrkB activation without affecting 5-HT_{2A} receptor functions. Importantly, these detrimental effects on TrkB functions were reversed by a pharmacological blockade of the 5-HT_{2A} receptor with ketanserin, a drug widely used to treat hypertension. Moreover, our data demonstrated that the stoichiometry of heterodimerization played a pivotal role in this process. This suggests that changes in the relative expression of both receptors and the corresponding changes in heterodimerization rates can provide an intriguing mechanism for the brain-region-specific regulation of TrkB functions in health and disease.

Author Contributions: T.I., E.P. and V.N. conceived the study. T.I., E.P. and V.N. designed the experiments. T.I., A.T., D.G., F.E.M. and V.N. conducted the experiments. T.I., F.E.M. and A.Z. analyzed the data. V.N., E.P. and S.B. contributed reagents, materials, and analytical tools. A.T. and T.I. wrote the manuscript. E.P. and V.N. edited the manuscript. All authors have read and agreed to the published version of the manuscript.

Funding: This research was supported by the DFG grants PO732 to Evgeni Ponimaskin, AZ994 to Andre Zeug and GU1521 to Daria Guseva and Russian Foundation for Basic Research grant 20-04-00253 to Tatiana V. Ilchibaeva. The animal maintenance was supported by the Basic Research Project FWNR-2022-0023.

Institutional Review Board Statement: The experimental procedures were conducted in accordance with the Guidelines for the Use of Animals in Neuroscience Research (2010), German law about animal protection, and European Communities Council Directive 86/609/EEC for the protection of animals used for experimental purposes and was approved by the ethical committee of The Institute of Cytology and Genetics (Protocol No. 33, 15 June 2016) and the Local Institutional Animal Care and Research Advisory committee (University of Hohenheim) with the permission of the local government (T 183/19 EM).

Informed Consent Statement: Not applicable.

Data Availability Statement: Data supporting the findings of this study are available from the corresponding authors on reasonable request.

Acknowledgments: We thank Tania Bunke and Dalia Abdel-Galil for the excellent technical support. Tatiana Ilchibaeva thanks IBRO-PERC, which provided the InEurope Short Stay Grant supporting her training in Evgeni Ponimaskin's lab at Hannover Medical School, Hannover, Germany.

Conflicts of Interest: The authors declare no conflict of interest.

References

1. Seroogy, K.B.; Lundgren, K.H.; Tran, T.M.; Guthrie, K.M.; Isackson, P.J.; Gall, C.M. Dopaminergic Neurons in Rat Ventral Midbrain Express Brain-Derived Neurotrophic Factor and Neurotrophin-3 MRNAs. *J. Comp. Neurol.* **1994**, *342*, 321–334. [CrossRef] [PubMed]
2. Ohira, K.; Hayashi, M. Expression of TrkB Subtypes in the Adult Monkey Cerebellar Cortex. *J. Chem. Neuroanat.* **2003**, *25*, 175–183. [CrossRef]
3. Tang, S.; Machaalani, R.; Waters, K.A. Immunolocalization of Pro- and Mature-Brain Derived Neurotrophic Factor (BDNF) and Receptor TrkB in the Human Brainstem and Hippocampus. *Brain Res.* **2010**, *1354*, 1–14. [CrossRef] [PubMed]
4. Baydyuk, M.; Xu, B. BDNF Signaling and Survival of Striatal Neurons. *Front. Cell. Neurosci.* **2014**, *8*, 254. [CrossRef] [PubMed]
5. Liao, G.-Y.; Kinney, C.E.; An, J.J.; Xu, B. TrkB-Expressing Neurons in the Dorsomedial Hypothalamus Are Necessary and Sufficient to Suppress Homeostatic Feeding. *Proc. Natl. Acad. Sci. USA* **2019**, *116*, 3256–3261. [CrossRef]
6. Jin, W. Regulation of BDNF-TrkB Signaling and Potential Therapeutic Strategies for Parkinson's Disease. *J. Clin. Med.* **2020**, *9*, 257. [CrossRef]
7. Huang, E.J.; Reichardt, L.F. Trk Receptors: Roles in Neuronal Signal Transduction. *Annu. Rev. Biochem.* **2003**, *72*, 609–642. [CrossRef]
8. Minichiello, L. TrkB Signalling Pathways in LTP and Learning. *Nat. Rev. Neurosci.* **2009**, *10*, 850–860. [CrossRef]
9. von Bohlen Und Halbach, O.; von Bohlen Und Halbach, V. BDNF Effects on Dendritic Spine Morphology and Hippocampal Function. *Cell Tissue Res.* **2018**, *373*, 729–741. [CrossRef]
10. Zagrebelsky, M.; Tacke, C.; Korte, M. BDNF Signaling during the Lifetime of Dendritic Spines. *Cell Tissue Res.* **2020**, *382*, 185–199. [CrossRef]
11. Björkholm, C.; Monteggia, L.M. BDNF—A Key Transducer of Antidepressant Effects. *Neuropharmacology* **2016**, *102*, 72–79. [CrossRef]
12. Rantamäki, T. TrkB Neurotrophin Receptor at the Core of Antidepressant Effects, but How? *Cell Tissue Res.* **2019**, *377*, 115–124. [CrossRef]
13. Xu, T.; Pandey, S.C. Cellular Localization of Serotonin(2A) (5HT(2A)) Receptors in the Rat Brain. *Brain Res. Bull.* **2000**, *51*, 499–505. [CrossRef]
14. Varnäs, K.; Halldin, C.; Hall, H. Autoradiographic Distribution of Serotonin Transporters and Receptor Subtypes in Human Brain. *Hum. Brain Mapp.* **2004**, *22*, 246–260. [CrossRef]
15. Béïque, J.-C.; Imad, M.; Mladenovic, L.; Gingrich, J.A.; Andrade, R. Mechanism of the 5-Hydroxytryptamine 2A Receptor-Mediated Facilitation of Synaptic Activity in Prefrontal Cortex. *Proc. Natl. Acad. Sci. USA* **2007**, *104*, 9870–9875. [CrossRef]
16. García-Oscos, F.; Torres-Ramírez, O.; Dinh, L.; Galindo-Charles, L.; Pérez Padilla, E.A.; Pineda, J.C.; Atzori, M.; Salgado, H. Activation of 5-HT Receptors Inhibits GABAergic Transmission by Pre- and Post-Synaptic Mechanisms in Layer II/III of the Juvenile Rat Auditory Cortex. *Synapse* **2015**, *69*, 115–127. [CrossRef]
17. Carhart-Harris, R.L.; Nutt, D.J. Serotonin and Brain Function: A Tale of Two Receptors. *J. Psychopharmacol.* **2017**, *31*, 1091–1120. [CrossRef]
18. Moravčíková, L.; Csatlósová, K.; Ďurišová, B.; Ondáčová, K.; Pavlovičová, M.; Lacinová, Ľ.; Dremencov, E. Role of Serotonin-2A Receptors in Pathophysiology and Treatment of Depression. *Receptors* **2018**, *32*, 205–230. [CrossRef]
19. Celada, P.; Puig, M.; Amargós-Bosch, M.; Adell, A.; Artigas, F. The Therapeutic Role of 5-HT_{1A} and 5-HT_{2A} Receptors in Depression. *J. Psychiatry Neurosci.* **2004**, *29*, 252–265.
20. McIntyre, R.S.; Soczynska, J.K.; Woldeyohannes, H.O.; Alsuwaidan, M.; Konarski, J.Z. A Preclinical and Clinical Rationale for Quetiapine in Mood Syndromes. *Expert Opin. Pharmacother.* **2007**, *8*, 1211–1219. [CrossRef]
21. Sanford, M.; Keating, G.M. Quetiapine: A Review of Its Use in the Management of Bipolar Depression. *CNS Drugs* **2012**, *26*, 435–460. [CrossRef]
22. Mestre, T.A.; Zurowski, M.; Fox, S.H. 5-Hydroxytryptamine 2A Receptor Antagonists as Potential Treatment for Psychiatric Disorders. *Expert Opin. Investig. Drugs* **2013**, *22*, 411–421. [CrossRef]
23. Wright, B.M.; Eiland, E.H., 3rd; Lorenz, R. Augmentation with Atypical Antipsychotics for Depression: A Review of Evidence-Based Support from the Medical Literature. *Pharmacotherapy* **2013**, *33*, 344–359. [CrossRef]
24. de Miranda, A.S.; Moreira, F.A.; Teixeira, A.L. The Preclinical Discovery and Development of Quetiapine for the Treatment of Mania and Depression. *Expert Opin. Drug Discov.* **2017**, *12*, 525–535. [CrossRef]
25. Tao, X.; Finkbeiner, S.; Arnold, D.B.; Shaywitz, A.J.; Greenberg, M.E. Ca^{2+} Influx Regulates BDNF Transcription by a CREB Family Transcription Factor-Dependent Mechanism. *Neuron* **1998**, *20*, 709–726. [CrossRef]
26. Vaidya, V.A.; Marek, G.J.; Aghajanian, G.K.; Duman, R.S. 5-HT_{2A} Receptor-Mediated Regulation of Brain-Derived Neurotrophic Factor MRNA in the Hippocampus and the Neocortex. *J. Neurosci.* **1997**, *17*, 2785–2795. [CrossRef]
27. Popova, N.K.; Ilchibaeva, T.V.; Naumenko, V.S. Neurotrophic Factors (BDNF and GDNF) and the Serotonergic System of the Brain. *Biochemistry* **2017**, *82*, 308–317. [CrossRef]
28. Jaggar, M.; Vaidya, V.A. 5-HT_{2A} Receptors and BDNF Regulation: Implications for Psychopathology. In *5-HT_{2A} Receptors in the Central Nervous System*; Humana Press: Cham, Switzerland, 2018; Volume 32, ISBN 9783319704746.
29. Popova, N.K.; Naumenko, V.S. Neuronal and Behavioral Plasticity: The Role of Serotonin and BDNF Systems Tandem. *Expert Opin. Ther. Targets* **2019**, *23*, 227–239. [CrossRef]

30. Borroto-Escuela, D.O.; Li, X.; Tarakanov, A.O.; Savelli, D.; Narváez, M.; Shumilov, K.; Andrade-Talavera, Y.; Jimenez-Beristain, A.; Pomierny, B.; Díaz-Cabiale, Z.; et al. Existence of Brain 5-HT_{1A}-5-HT_{2A} Isoreceptor Complexes with Antagonistic Allosteric Receptor-Receptor Interactions Regulating 5-HT_{1A} Receptor Recognition. *ACS Omega* **2017**, *2*, 4779–4789. [CrossRef]
31. Lukasiewicz, S.; Polit, A.; Kędracka-Krok, S.; Wędzony, K.; Maćkowiak, M.; Dziedzicka-Wasylewska, M. Hetero-Dimerization of Serotonin 5-HT(2A) and Dopamine D(2) Receptors. *Biochim. Biophys. Acta* **2010**, *1803*, 1347–1358. [CrossRef]
32. Moreno, J.L.; Muguruza, C.; Umali, A.; Mortillo, S.; Holloway, T.; Pilar-Cuéllar, F.; Mocci, G.; Seto, J.; Callado, L.F.; Neve, R.L.; et al. Identification of Three Residues Essential for 5-Hydroxytryptamine 2A-Metabotropic Glutamate 2 (5-HT_{2A}·mGlu2) Receptor Heteromerization and Its Psychoactive Behavioral Function. *J. Biol. Chem.* **2012**, *287*, 44301–44319. [CrossRef] [PubMed]
33. Sonnenberg, S.B.; Rauer, J.; Göhr, C.; Gorinski, N.; Schade, S.K.; Abdel Galil, D.; Naumenko, V.; Zeug, A.; Bischoff, S.C.; Ponimaskin, E.; et al. The 5-HT(4) Receptor Interacts with Adhesion Molecule L1 to Modulate Morphogenic Signaling in Neurons. *J. Cell Sci.* **2021**, *134*, jcs249193. [CrossRef] [PubMed]
34. Labus, J.; Röhrs, K.-F.; Ackmann, J.; Varbanov, H.; Müller, F.E.; Jia, S.; Jahreis, K.; Vollbrecht, A.-L.; Butzlaff, M.; Schill, Y.; et al. Amelioration of Tau Pathology and Memory Deficits by Targeting 5-HT7 Receptor. *Prog. Neurobiol.* **2021**, *197*, 101900. [CrossRef] [PubMed]
35. Bijata, M.; Labus, J.; Guseva, D.; Stawarski, M.; Butzlaff, M.; Dzwonek, J.; Schneeberg, J.; Böhm, K.; Michaluk, P.; Rusakov, D.A.; et al. Synaptic Remodeling Depends on Signaling between Serotonin Receptors and the Extracellular Matrix. *Cell Rep.* **2017**, *19*, 1767–1782. [CrossRef]
36. Jang, S.-W.; Liu, X.; Yepes, M.; Shepherd, K.R.; Miller, G.W.; Liu, Y.; Wilson, W.D.; Xiao, G.; Blanchi, B.; Sun, Y.E.; et al. A Selective TrkB Agonist with Potent Neurotrophic Activities by 7,8-Dihydroxyflavone. *Proc. Natl. Acad. Sci. USA* **2010**, *107*, 2687–2692. [CrossRef]
37. Halberstadt, A.L.; Sindhunata, I.S.; Scheffers, K.; Flynn, A.D.; Sharp, R.F.; Geyer, M.A.; Young, J.W. Effect of 5-HT_{2A} and 5-HT2C Receptors on Temporal Discrimination by Mice. *Neuropharmacology* **2016**, *107*, 364–375. [CrossRef]
38. Meller, R.; Harrison, P.J.; Elliott, J.M.; Sharp, T. In Vitro Evidence That 5-Hydroxytryptamine Increases Efflux of Glial Glutamate via 5-HT(2A) Receptor Activation. *J. Neurosci. Res.* **2002**, *67*, 399–405. [CrossRef]
39. Renner, U.; Zeug, A.; Woehler, A.; Niebert, M.; Dityatev, A.; Dityateva, G.; Gorinski, N.; Guseva, D.; Abdel-Galil, D.; Fröhlich, M.; et al. Heterodimerization of Serotonin Receptors 5-HT_{1A} and 5-HT7 Differentially Regulates Receptor Signalling and Trafficking. *J. Cell Sci.* **2012**, *125*, 2486–2499. [CrossRef]
40. Wlodarczyk, J.; Woehler, A.; Kobe, F.; Ponimaskin, E.; Zeug, A.; Neher, E. Analysis of FRET Signals in the Presence of Free Donors and Acceptors. *Biophys. J.* **2008**, *94*, 986–1000. [CrossRef]
41. Prasad, S.; Zeug, A.; Ponimaskin, E. Analysis of Receptor-Receptor Interaction by Combined Application of FRET and Microscopy. *Methods Cell Biol.* **2013**, *117*, 243–265. [CrossRef]
42. Kulikov, A.V.; Naumenko, V.S.; Voronova, I.P.; Tikhonova, M.A.; Popova, N.K. Quantitative RT-PCR Assay of 5-HT_{1A} and 5-HT_{2A} Serotonin Receptor MRNAs Using Genomic DNA as an External Standard. *J. Neurosci. Methods* **2005**, *141*, 97–101. [CrossRef]
43. Naumenko, V.S.; Kulikov, A.V. Quantitative assay of 5-HT(1A) serotonin receptor gene expression in the brain. *Mol. Biol.* **2006**, *40*, 37–44. [CrossRef]
44. Naumenko, V.S.; Osipova, D.V.; Kostina, E.V.; Kulikov, A.V. Utilization of a Two-Standard System in Real-Time PCR for Quantification of Gene Expression in the Brain. *J. Neurosci. Methods* **2008**, *170*, 197–203. [CrossRef]
45. Guo, H.; An, S.; Ward, R.; Yang, Y.; Liu, Y.; Guo, X.-X.; Hao, Q.; Xu, T.-R. Methods Used to Study the Oligomeric Structure of G-Protein-Coupled Receptors. *Biosci. Rep.* **2017**, *37*, BSR20160547. [CrossRef]
46. Dorsch, S.; Klotz, K.-N.; Engelhardt, S.; Lohse, M.J.; Bünemann, M. Analysis of Receptor Oligomerization by FRAP Microscopy. *Nat. Methods* **2009**, *6*, 225–230. [CrossRef]
47. Taura, J.; Fernández-Dueñas, V.; Ciruela, F. Visualizing G Protein-Coupled Receptor-Receptor Interactions in Brain Using Proximity Ligation In Situ Assay. *Curr. Protoc. Cell Biol.* **2015**, *67*, 17.17.1–17.17.16. [CrossRef]
48. Shang, W.; Lu, F.; Sun, T.; Xu, J.; Li, L.-L.; Wang, Y.; Wang, G.; Chen, L.; Wang, X.; Cannell, M.B.; et al. Imaging Ca^{2+} Nanosparks in Heart with a New Targeted Biosensor. *Circ. Res.* **2014**, *114*, 412–420. [CrossRef]
49. Müller, F.E.; Cherkas, V.; Stopper, G.; Caudal, L.C.; Stopper, L.; Kirchhoff, F.; Henneberger, C.; Ponimaskin, E.G.; Zeug, A. Elucidating Regulators of Astrocytic Ca^{2+} Signaling via Multi-Threshold Event Detection (MTED). *Glia* **2021**, *69*, 2798–2811. [CrossRef]
50. Roth, B.L.; Palvimaki, E.P.; Berry, S.; Khan, N.; Sachs, N.; Uluer, A.; Choudhary, M.S. 5-Hydroxytryptamine2A (5-HT_{2A}) Receptor Desensitization Can Occur without down-Regulation. *J. Pharmacol. Exp. Ther.* **1995**, *275*, 1638–1646.
51. Saucier, C.; Albert, P.R. Identification of an Endogenous 5-Hydroxytryptamine2A Receptor in NIH-3T3 Cells: Agonist-Induced down-Regulation Involves Decreases in Receptor RNA and Number. *J. Neurochem.* **1997**, *68*, 1998–2011. [CrossRef]
52. Aloyo, V.J.; Berg, K.A.; Spampinato, U.; Clarke, W.P.; Harvey, J.A. Current Status of Inverse Agonism at Serotonin2A (5-HT_{2A}) and 5-HT2C Receptors. *Pharmacol. Ther.* **2009**, *121*, 160–173. [CrossRef]
53. Yoshii, A.; Murata, Y.; Kim, J.; Zhang, C.; Shokat, K.M.; Constantine-Paton, M. TrkB and Protein Kinase Mζ Regulate Synaptic Localization of PSD-95 in Developing Cortex. *J. Neurosci.* **2011**, *31*, 11894–11904. [CrossRef]
54. Liu, C.; Chan, C.B.; Ye, K. 7,8-Dihydroxyflavone, a Small Molecular TrkB Agonist, Is Useful for Treating Various BDNF-Implicated Human Disorders. *Transl. Neurodegener.* **2016**, *5*, 2. [CrossRef]

55. Ly, C.; Greb, A.C.; Cameron, L.P.; Wong, J.M.; Barragan, E.V.; Wilson, P.C.; Burbach, K.F.; Soltanzadeh Zarandi, S.; Sood, A.; Paddy, M.R.; et al. Psychedelics Promote Structural and Functional Neural Plasticity. *Cell Rep.* **2018**, *23*, 3170–3182. [CrossRef]
56. Tsybko, A.S.; Ilchibaeva, T.V.; Filimonova, E.A.; Eremin, D.V.; Popova, N.K.; Naumenko, V.S. The Chronic Treatment With 5-HT_{2A} Receptor Agonists Affects the Behavior and the BDNF System in Mice. *Neurochem. Res.* **2020**, *45*, 3059–3075. [CrossRef]
57. Flajolet, M.; Wang, Z.; Futter, M.; Shen, W.; Nuangchamnong, N.; Bendor, J.; Wallach, I.; Nairn, A.C.; Surmeier, D.J.; Greengard, P. FGF Acts as a Co-Transmitter through Adenosine A(2A) Receptor to Regulate Synaptic Plasticity. *Nat. Neurosci.* **2008**, *11*, 1402–1409. [CrossRef]
58. Di Palma, M.; Sartini, S.; Lattanzi, D.; Cuppini, R.; Pita-Rodriguez, M.; Diaz-Carmenate, Y.; Narvaez, M.; Fuxe, K.; Borroto-Escuela, D.O.; Ambrogini, P. Evidence for the Existence of A2AR-TrkB Heteroreceptor Complexes in the Dorsal Hippocampus of the Rat Brain: Potential Implications of A2AR and TrkB Interplay upon Ageing. *Mech. Ageing Dev.* **2020**, *190*, 111289. [CrossRef]
59. Borroto-Escuela, D.O.; Romero-Fernandez, W.; Mudó, G.; Pérez-Alea, M.; Ciruela, F.; Tarakanov, A.O.; Narvaez, M.; Di Liberto, V.; Agnati, L.F.; Belluardo, N.; et al. Fibroblast Growth Factor Receptor 1-5-Hydroxytryptamine 1A Heteroreceptor Complexes and Their Enhancement of Hippocampal Plasticity. *Biol. Psychiatry* **2012**, *71*, 84–91. [CrossRef]
60. Dwivedi, Y.; Rizavi, H.S.; Conley, R.R.; Roberts, R.C.; Tamminga, C.A.; Pandey, G.N. Altered Gene Expression of Brain-Derived Neurotrophic Factor and Receptor Tyrosine Kinase B in Postmortem Brain of Suicide Subjects. *Arch. Gen. Psychiatry* **2003**, *60*, 804–815. [CrossRef]
61. Pandey, G.N.; Ren, X.; Rizavi, H.S.; Conley, R.R.; Roberts, R.C.; Dwivedi, Y. Brain-Derived Neurotrophic Factor and Tyrosine Kinase B Receptor Signalling in Post-Mortem Brain of Teenage Suicide Victims. *Int. J. Neuropsychopharmacol.* **2008**, *11*, 1047–1061. [CrossRef]
62. Banerjee, R.; Ghosh, A.K.; Ghosh, B.; Bhattacharyya, S.; Mondal, A.C. Decreased MRNA and Protein Expression of BDNF, NGF, and Their Receptors in the Hippocampus from Suicide: An Analysis in Human Postmortem Brain. *Clin. Med. Insights Pathol.* **2013**, *6*, 1–11. [CrossRef] [PubMed]
63. Dwivedi, Y.; Rizavi, H.S.; Zhang, H.; Mondal, A.C.; Roberts, R.C.; Conley, R.R.; Pandey, G.N. Neurotrophin Receptor Activation and Expression in Human Postmortem Brain: Effect of Suicide. *Biol. Psychiatry* **2009**, *65*, 319–328. [CrossRef] [PubMed]
64. Stockmeier, C.A. Involvement of Serotonin in Depression: Evidence from Postmortem and Imaging Studies of Serotonin Receptors and the Serotonin Transporter. *J. Psychiatr. Res.* **2003**, *37*, 357–373. [CrossRef]
65. Bach, H.; Arango, V. Neuroanatomy of Serotonergic Abnormalities in Suicide. In *the Neurobiological Basis of Suicide*; Dwivedi, Y., Ed.; Taylor & Francis Group, LLC.: Boca Raton, FL, USA, 2012; ISBN 978-1-4398-3881-5.
66. Pandey, G.N.; Dwivedi, Y.; Rizavi, H.S.; Ren, X.; Pandey, S.C.; Pesold, C.; Roberts, R.C.; Conley, R.R.; Tamminga, C.A. Higher Expression of Serotonin 5-HT(2A) Receptors in the Postmortem Brains of Teenage Suicide Victims. *Am. J. Psychiatry* **2002**, *159*, 419–429. [CrossRef]
67. Cahir, M.; Ardis, T.; Reynolds, G.P.; Cooper, S.J. Acute and Chronic Tryptophan Depletion Differentially Regulate Central 5-HT_{1A} and 5-HT_{2A} Receptor Binding in the Rat. *Psychopharmacology* **2007**, *190*, 497–506. [CrossRef]
68. Jennings, K.A.; Sheward, W.J.; Harmar, A.J.; Sharp, T. Evidence That Genetic Variation in 5-HT Transporter Expression Is Linked to Changes in 5-HT_{2A} Receptor Function. *Neuropharmacology* **2008**, *54*, 776–783. [CrossRef]
69. Jørgensen, L.M.; Weikop, P.; Villadsen, J.; Visnapuu, T.; Ettrup, A.; Hansen, H.D.; Baandrup, A.O.; Andersen, F.L.; Bjarkam, C.R.; Thomsen, C.; et al. Cerebral 5-HT Release Correlates with [(11)C]Cimbi36 PET Measures of 5-HT_{2A} Receptor Occupancy in the Pig Brain. *J. Cereb. Blood Flow Metab.* **2017**, *37*, 425–434. [CrossRef]
70. Di Lieto, A.; Rantamäki, T.; Vesa, L.; Yanpallewar, S.; Antila, H.; Lindholm, J.; Rios, M.; Tessarollo, L.; Castrén, E. The Responsiveness of TrkB to BDNF and Antidepressant Drugs Is Differentially Regulated during Mouse Development. *PLoS ONE* **2012**, *7*, e32869. [CrossRef]
71. Autry, A.E.; Monteggia, L.M. Brain-Derived Neurotrophic Factor and Neuropsychiatric Disorders. *Pharmacol. Rev.* **2012**, *64*, 238–258. [CrossRef]
72. Castrén, E.; Antila, H. Neuronal Plasticity and Neurotrophic Factors in Drug Responses. *Mol. Psychiatry* **2017**, *22*, 1085–1095. [CrossRef]
73. Diniz, C.R.A.F.; Casarotto, P.C.; Resstel, L.; Joca, S.R.L. Beyond Good and Evil: A Putative Continuum-Sorting Hypothesis for the Functional Role of ProBDNF/BDNF-Propeptide/MBDNF in Antidepressant Treatment. *Neurosci. Biobehav. Rev.* **2018**, *90*, 70–83. [CrossRef]
74. Carr, G.V.; Lucki, I. The Role of Serotonin Receptor Subtypes in Treating Depression: A Review of Animal Studies. *Psychopharmacology* **2011**, *213*, 265–287. [CrossRef]
75. Pandey, D.K.; Bhatt, S.; Jindal, A.; Gautam, B. Effect of Combination of Ketanserin and Escitalopram on Behavioral Anomalies after Olfactory Bulbectomy: Prediction of Quick Onset of Antidepressant Action. *Indian J. Pharmacol.* **2014**, *46*, 639–643. [CrossRef]
76. Muguruza, C.; Miranda-Azpiazu, P.; Díez-Alarcia, R.; Morentin, B.; González-Maeso, J.; Callado, L.F.; Meana, J.J. Evaluation of 5-HT_{2A} and MGlu2/3 Receptors in Postmortem Prefrontal Cortex of Subjects with Major Depressive Disorder: Effect of Antidepressant Treatment. *Neuropharmacology* **2014**, *86*, 311–318. [CrossRef]
77. Guiard, B.P.; Di Giovanni, G. Central Serotonin-2A (5-HT_{2A}) Receptor Dysfunction in Depression and Epilepsy: The Missing Link? *Front. Pharmacol.* **2015**, *6*, 46. [CrossRef]
78. Jha, S.; Rajendran, R.; Fernandes, K.A.; Vaidya, V.A. 5-HT_{2A}/2C Receptor Blockade Regulates Progenitor Cell Proliferation in the Adult Rat Hippocampus. *Neurosci. Lett.* **2008**, *441*, 210–214. [CrossRef]

79. Pilar-Cuéllar, F.; Vidal, R.; Pazos, A. Subchronic Treatment with Fluoxetine and Ketanserin Increases Hippocampal Brain-Derived Neurotrophic Factor, β-Catenin and Antidepressant-like Effects. *Br. J. Pharmacol.* **2012**, *165*, 1046–1057. [CrossRef]
80. Chlan-Fourney, J.; Ashe, P.; Nylen, K.; Juorio, A.V.; Li, X.M. Differential Regulation of Hippocampal BDNF MRNA by Typical and Atypical Antipsychotic Administration. *Brain Res.* **2002**, *954*, 11–20. [CrossRef]
81. Bai, O.; Chlan-Fourney, J.; Bowen, R.; Keegan, D.; Li, X.-M. Expression of Brain-Derived Neurotrophic Factor MRNA in Rat Hippocampus after Treatment with Antipsychotic Drugs. *J. Neurosci. Res.* **2003**, *71*, 127–131. [CrossRef]
82. Seo, M.K.; Lee, C.H.; Cho, H.Y.; You, Y.S.; Lee, B.J.; Lee, J.G.; Park, S.W.; Kim, Y.H. Effects of Antipsychotic Drugs on the Expression of Synapse-Associated Proteins in the Frontal Cortex of Rats Subjected to Immobilization Stress. *Psychiatry Res.* **2015**, *229*, 968–974. [CrossRef]
83. Fumagalli, F.; Molteni, R.; Bedogni, F.; Gennarelli, M.; Perez, J.; Racagni, G.; Riva, M.A. Quetiapine Regulates FGF-2 and BDNF Expression in the Hippocampus of Animals Treated with MK-801. *Neuroreport* **2004**, *15*, 2109–2112. [CrossRef]
84. Angelucci, F.; Aloe, L.; Iannitelli, A.; Gruber, S.H.M.; Mathé, A.A. Effect of Chronic Olanzapine Treatment on Nerve Growth Factor and Brain-Derived Neurotrophic Factor in the Rat Brain. *Eur. Neuropsychopharmacol.* **2005**, *15*, 311–317. [CrossRef]
85. Xu, H.; Chen, Z.; He, J.; Haimanot, S.; Li, X.; Dyck, L.; Li, X.-M. Synergetic Effects of Quetiapine and Venlafaxine in Preventing the Chronic Restraint Stress-Induced Decrease in Cell Proliferation and BDNF Expression in Rat Hippocampus. *Hippocampus* **2006**, *16*, 551–559. [CrossRef]
86. Park, S.-W.; Lee, S.-K.; Kim, J.-M.; Yoon, J.-S.; Kim, Y.-H. Effects of Quetiapine on the Brain-Derived Neurotrophic Factor Expression in the Hippocampus and Neocortex of Rats. *Neurosci. Lett.* **2006**, *402*, 25–29. [CrossRef]
87. Pillai, A.; Terry, A.V.J.; Mahadik, S.P. Differential Effects of Long-Term Treatment with Typical and Atypical Antipsychotics on NGF and BDNF Levels in Rat Striatum and Hippocampus. *Schizophr. Res.* **2006**, *82*, 95–106. [CrossRef]
88. Balu, D.T.; Hoshaw, B.A.; Malberg, J.E.; Rosenzweig-Lipson, S.; Schechter, L.E.; Lucki, I. Differential Regulation of Central BDNF Protein Levels by Antidepressant and Non-Antidepressant Drug Treatments. *Brain Res.* **2008**, *1211*, 37–43. [CrossRef]
89. Kim, H.-W.; Cheon, Y.; Modi, H.R.; Rapoport, S.I.; Rao, J.S. Effects of Chronic Clozapine Administration on Markers of Arachidonic Acid Cascade and Synaptic Integrity in Rat Brain. *Psychopharmacology* **2012**, *222*, 663–674. [CrossRef]
90. Park, S.W.; Lee, C.H.; Cho, H.Y.; Seo, M.K.; Lee, J.G.; Lee, B.J.; Seol, W.; Kee, B.S.; Kim, Y.H. Effects of Antipsychotic Drugs on the Expression of Synaptic Proteins and Dendritic Outgrowth in Hippocampal Neuronal Cultures. *Synapse* **2013**, *67*, 224–234. [CrossRef]